Published in final edited form as:
Dev Dyn. 2010 December ; 239(12): 3303–3311. doi:10.1002/dvdy.22449.

Expression of *Slit* and *Robo* Genes in the Developing Mouse Heart

Caroline Medioni[1], **Nicolas Bertrand**[2], **Karim Mesbah**[3], **Bruno Hudry**[3], **Laurent Dupays**[4], **Orit Wolstein**[5], **Andrew J. Washkowitz**[6], **Virginia E. Papaioannou**[6], **Timothy J. Mohun**[4], **Richard P. Harvey**[5,7], and **Stéphane Zaffran**[2,*]

[1]Institute of Developmental Biology and Cancer, CNRS UMR 6543, Faculté des Sciences, Parc Valrose Nice, France

[2]Inserm UMR_S910, Université de la Méditerranée, Faculté de Médecine de la Timone, Marseille, France

[3]Developmental Biology Institute of Marseille-Luminy, CNRS UMR 6216, Université de la Méditerranée, Campus de Luminy Case 907, Marseille, France

[4]Division of Developmental Biology, MRC National Institute for Medical Research, The Ridgeway, Mill Hill, London, United Kingdom

[5]Victor Chang Cardiac Research Institute, Sydney, Australia

[6]Department of Genetics and Development, Columbia University Medical Center, New York, New York

[7]Faculties of Life Sciences and Medicine, University of New South Wales, Kensington, Australia

Abstract

Development of the mammalian heart is mediated by complex interactions between myocardial, endocardial, and neural crest-derived cells. Studies in *Drosophila* have shown that the Slit-Robo signaling pathway controls cardiac cell shape changes and lumen formation of the heart tube. Here, we demonstrate by in situ hybridization that multiple Slit ligands and Robo receptors are expressed in the developing mouse heart. *Slit3* is the predominant ligand transcribed in the early mouse heart and is expressed in the ventral wall of the linear heart tube and subsequently in chamber but not in atrioventricular canal myocardium. Furthermore, we identify that the homeobox gene *Nkx2-5* is required for early ventral restriction of *Slit3* and that the T-box transcription factor Tbx2 mediates repression of *Slit3* in nonchamber myocardium. Our results suggest that patterned Slit-Robo signaling may contribute to the control of oriented cell growth during chamber morphogenesis of the mammalian heart.

Keywords

Slit/Robo pathway; cardiac development; mouse; Tbx; atrioventricular canal

*Correspondence to: Stéphane Zaffran, Inserm UMR_S910, Faculté de Médecine de la Timone, 27 Bd Jean Moulin, 13005 Marseille, France. stephane.zaffran@univmed.fr.
Drs. Medioni and Bertrand contributed equally to this work.

INTRODUCTION

Cardiogenesis is one of the earliest and most critical steps during vertebrate organogenesis. Heart development begins when cardiac progenitor cells in the anterior lateral mesoderm cluster in the primary heart field (Harvey, 2002). These cells give rise to the cardiac crescent and linear heart tube containing the future left ventricle and atrioventricular canal (AVC; see Buckingham et al., 2005). Subsequently the heart tube undergoes rightward looping (Harvey, 2002). As looping progresses, cells of the second heart field in splanchnic mesoderm are added to the heart tube to form the outflow tract (OFT), right ventricle, atria and inflow tract regions (Buckingham et al., 2005). Subsequently, atrial and ventricular chambers form through a localized process that involves differential growth or "ballooning" of the outer curvature of the heart tube (Christoffels et al., 2000). Importantly, part of the heart tube, including the OFT, inner curvature, AVC, and inflow tract, escapes this developmental chamber program through the repressive action of the T-box factors, Tbx2 and Tbx3 (Habets et al., 2002; Christoffels et al., 2004b; Harrelson et al., 2004; Bakker et al., 2008). Regionalized gene expression provides evidence for the presence of dorsoventral patterning in the early tube that precedes chamber development (Christoffels et al., 2004a). A retrospective clonal analysis of cardiac cells has shown that myocardium, from the time of its formation, is a polarized and regionalized tissue in which oriented cell growth may be important in shaping the chambers (Meilhac et al., 2004). Although key factors that play a role in forming the heart tube have been identified, including GATA4, NKX2-5, dHAND, TBX5, or RALDH2 (Harvey, 2002), the molecular effectors of cell polarity and cell shape changes remain unknown.

The extracellular-matrix molecule Slit and its Robo (roundabout) family receptors have been implicated in the regulation of cell polarity and morphogenesis during formation of the cardiac tube in *Drosophila* (Qian et al., 2005; MacMullin and Jacobs, 2006; Medioni et al., 2008; Santiago-Martinez et al., 2008). In particular, the Slit-Robo pathway is required for progressive polarization of cardiac cells during migration to the midline (Medioni et al., 2008). In contrast to the single *Slit* and three *Robo* genes in *Drosophila*, three distinct *Slit* genes (*Slit1, Slit2*, and *Slit3*) and four distinct *Robo* genes (*Robo1, Robo2, Rig1/Robo3*, and *Robo4*) are found in mammals (Chedotal, 2007). Slit functions as a repulsive ligand for the Robo-family receptors in the central nervous system (CNS), and acts both attractively and repulsively in somatic muscles (Kidd et al., 1998, 1999; Brose et al., 1999; Simpson et al., 2000; Wu et al., 2001). In addition, both gene families display distinct expression patterns outside the CNS (Holmes et al., 1998; Yuan et al., 1999; Strickland et al., 2006). Remarkably, *Slit3* is widely expressed in different organs, including the tongue, kidney, pharynx, umbilical cord vein, heart, lung, and diaphragm (Yuan et al., 1999; Liu et al., 2003; Yuan et al., 2003). Consistent with its expression in non-neural tissues, studies have established that Slit3 is required for angiogenesis and formation of the diaphragm and kidney (Liu et al., 2003; Yuan et al., 2003; Zhang et al., 2009).

The role of the *Drosophila* Slit-Robo pathway in regulating changes in cell shape during cardiac tube formation prompted us to conduct a detailed analysis of murine *Slit* and *Robo* gene expression during mouse heart development. We describe that *Slit3* in particular, shows a specific localization in the ventral region of the forming heart tube and subsequently restriction to chamber myocardium. We show that the homeobox gene *Nkx2-5* is required for the ventral restriction of *Slit3* in the linear heart tube. In addition, we demonstrate that the T-box factors Tbx2 and Tbx20 mediate the restriction of *Slit3* expression to the chamber myocardium. Given the spatial and temporal expression profile of *Slit3* and its role in polarized growth and migration in other tissues, we propose that Slit-Robo signaling may be required for cardiac chamber expansion.

RESULTS AND DISCUSSION

Expression of Mouse *Slit* and *Robo* Genes During Heart Development

Previous studies in *Drosophila* have shown that the Slit-Robo signaling pathway controls cardiac cell polarity and formation of the cardiac lumen (Medioni et al., 2009). Therefore, we decided to analyze the expression pattern of murine *Slit* and *Robo* genes in the developing heart. In contrast to other tissues, detailed analysis of the cardiac expression pattern of *Slit* and *Robo* genes has not been reported (Holmes et al., 1998; Yuan et al., 1999; Holmes and Niswander, 2001; Liu et al., 2003; Yuan et al., 2003). Mouse embryos between 7.5 and 12.5 days of development (E7.5–E12.5) were hybridized with antisense riboprobes for *Slit1, Slit2, Slit3, Robo1, Robo2, Rig1/Robo3*, and *Robo4* (Figs. 1, 2; also see Supp. Fig. S1, which is available online).

During this period of development, *Slit1* expression was primarily observed in the roof plate and the floor plate (Fig. 1A,B). *Slit1* transcripts were also observed in the mesodermal core of the pharyngeal arches (Fig. 1B,B′). Interestingly, pharyngeal mesoderm has been shown to contribute to the formation of the OFT as well as the pharyngeal arch artery (PAA) development (see Kelly and Buckingham, 2002). At E9.5, *Slit1* expression was detected in the developing heart in the left and right atria (Fig. 1C). However, at E12.5 we did not observe any expression in the heart (Fig. 1D,D′).

Similarly to *Slit1, Slit2* expression was observed prominently in neural tissue (Fig. 1E,F). From E8.5 to E9.5, *Slit2* expression was not detected in the myocardium; however, it was highly expressed in the pharyngeal region at these stages (Fig. 1F) as reported by others (Yuan et al., 1999; Calmont et al., 2009). Strong expression of *Slit2* was seen in the pharyngeal surface ectoderm (Fig. 1F′). This tissue has been shown to be a crucial source of signals for fourth PAA formation and remodeling (Kirby, 2007). *Slit2* has also been identified as a downstream target of Tbx1, and is implicated in cardiac neural crest cells (NCC) migration at the time of PAA formation (Calmont et al., 2009). While no clear expression in the embryonic heart was detected at E9.5 (Fig. 1G), a strong expression of *Slit2* was observed in the trabecular region of the ventricular chambers at E12.5 (Fig. 1H,H′). Of interest, the trabecular formation occurs when cardiomyocytes migrate toward the endocardium, which is coincident with upregulation of cell adhesion molecules (Ong et al., 1998). Thus, our observation suggests that other cell signaling molecules such as Slit may be involved in this process.

Slit3 is the earliest *Slit* gene to be expressed in the developing heart. Transcripts were observed in the cardiac crescent at E7.5 and in the linear heart tube at E8.5 (Fig. 1I,I′). At E8.5, *Slit3* expression is observed on the ventral wall of the linear heart tube (see Fig. 3A,B). *Slit3* is also expressed in the ventral midline and developing somites (Fig. 1I,J). Unlike the other *Slit* genes, *Slit3* expression was observed in all compartments of embryonic heart at E9.5, restricted to the outer curvature of the looped heart (Fig. 1J,K). The myocardium of the outer curvature is known to give rise to the ventricular chamber or “working” myocardium (de la Cruz and Markwald, 1999; Christoffels et al., 2000). Analysis of the distribution of clonally related myocytes has demonstrated that different patterns of oriented cell growth underlie regional differences in morphogenesis within the embryonic heart (Meilhac et al., 2004). The expression pattern of *Slit3* and its established role in polarized growth and migration in other tissues suggest implication of Slit-Robo signaling in the oriented cell growth that accompanies ballooning of the ventricular chambers (Christoffels et al., 2004a). By E12.5, expression of *Slit3* was observed only in myocardium of the atria and at the base of the great arteries (Fig. 1L,L′), in agreement with published expression data (Liu et al., 2003). Remarkably, during early heart development, *Slit2* and *Slit3* are both distributed within the ventricular chambers, suggesting requirement of a specific Slit ligand

during ventricular and trabecular formation of the embryonic heart. Despite that difference, *Slit2* and *Slit3* were detected in the surface pharyngeal ectoderm of embryo at E9.5 (Fig. 1F,F′,J,J′), suggesting redundancy of these molecules during cardiac NCC migration and PAA formation. The Slit-Robo signaling pathway is known to be involved in trunk neural crest migration (Jia et al., 2005). It would be interesting to identify whether Slit-Robo signaling mediates repulsive or attractive signals during cardiac NCC migration.

Robo family members Robo1-4 are the putative receptors for Slit ligands. Whereas *Robo4* is specifically expressed in the vascular endothelium (Supp. Fig. S1; Park et al., 2003), the expression profile of the three other members during heart development has not been analyzed in detail (Yuan et al., 1999; Camurri et al., 2004; Jia et al., 2005). In situ hybridization with *Robo1* and *Robo2* riboprobes showed that these receptors were both expressed in the venous pole of the linear heart tube at E8.5 (Fig. 2A,E). In agreement with a recent study (Calmont et al., 2009), we found *Robo1* expression in migrating NCCs (Fig. 2B). At E9.5, *Robo1* expression was faintly detected in the endocardial cushions of the OFT (Fig. 2C). Later, *Robo1* expression was maintained in the great arteries (Fig. 2D). Unlike other *Robo* genes, a consistent expression of *Robo2* was observed in both atria of the heart at E10.5 (Fig. 2G). At E12.5, *Robo2* expression was observed in the endocardium of the great arteries (Fig. 2H). The specific expression of *Slit* ligand and *Robo* receptor genes in the venous pole at E8.5 and in the atria from E9.5 to E12.5 suggests a role for these molecules in oriented cell growth and migration during atrial morphogenesis (Meilhac et al., 2004). Finally, from our in situ hybridization analysis we did not detect any expression of *Rig1/Robo3* and *Robo4* in the developing mouse heart at any time-point analyzed (Supp. Fig. S1).

Dorsoventral Patterning of *Slit3* Is Controlled by Nkx2-5

As noted above, whole-mount in situ hybridization analysis revealed expression of *Slit3* transcripts in the linear heart tube at E8.5 (Fig. 1I). At this stage, *Slit3* expression is comparable to the expression of the basic helix–loop–helix (bHLH) transcription factor gene, *Hand1*, which is restricted to the ventral wall of the forming heart tube (Fig. 3A–D; Biben and Harvey, 1997;Christoffels et al., 2000;Togi et al., 2004). Although *Slit3* is expressed at high levels in the developing heart, early cardiac defects have not been reported in *Slit3* mutant embryos (Liu et al., 2003;Yuan et al., 2003). However, the expression of *Slit3* detected in the outer curvature of the looped heart and the enlarged right ventricle observed in the hearts of *Slit3* mutant mice (Liu et al., 2003), suggest a role for Slit signaling in ventricular chamber formation. Further studies are required to determine whether subtle changes may exist in the heart of these mutants especially during the formation of the myocardium chambers and the great arteries.

We subsequently examined expression of *Slit3* in mutant mice affecting cardiac morphogenesis. Mutations in the NK-like homeobox gene, *Nkx2-5/Csx*, causes early embryonic lethality with cardiac development arrested at the linear heart tube stage, before looping (Komuro and Izumo, 1993; Lyons et al., 1995; Biben and Harvey, 1997). In *Nkx2-5*$^{-/-}$ embryos, the early expression of *Slit3* was indistinguishable from that in control embryos (Fig. 3E). However, we found that the dorsoventral pattern of *Slit3* expression in the linear heart tube was perturbed and expression was observed throughout the mutant heart tube (Fig. 3E,F). This result suggests that the myocardium of *Nkx2-5*$^{-/-}$ embryos is competent to express *Slit3* but not to interpret signals that restrict expression on the ventral side of the heart. Of note, two putative Nkx2-5 binding motifs (TGAAGTGATG and TAAAGTGGGT) are found in a 3,000 bp Slit3 5′ proximal fragment as predicted using the TFSEARCH program (http://mbs.cbcr.jp/research/db/TFSEARCH.html).

Expression of *Robo* receptor genes in the venous pole (Fig. 2A,E) incited us to examine their expression in *Nkx2-5*$^{-/-}$ embryos. Of interest, we did not detect expression of *Robo2* in the

linear heart tube of *Nkx2-5* mutant embryos (Supp. Fig. S2). This observation suggests that Nkx2-5 regulates in a different way *Slit* ligand and *Robo* receptor genes during the formation of the embryonic heart tube.

Regulation of the Chamber-Specific Expression Profile of *Slit3*

In looped hearts (E9–E9.5), *Slit3* expression was confined to the atrial and ventricular myocardium but was clearly absent from the AVC (Fig. 4A–C), a pattern resembling that of *atrial natriuretic factor* (*ANF*; see Supp. Fig. S3A), *Chisel*, and *Connexin40* at this stage (Christoffels et al., 2000). At E10.5 and E12.5 *Slit3* expression was restricted to the atria and the OFT (Figs. 1L, 4C–E). Immunohistochemistry revealed Slit3 protein expression in both atrial and ventricular myocardium at E10.5 (Fig. 4F). The AVC region was negative, confirming our results by in situ hybridization. Detection of Slit3 protein but not mRNA in the ventricles of the heart at E10.5 (Fig. 4E,F) indicates a persistence of the protein in the chamber myocardium. Although *Slit3* expression overlaps with *Robo1* and *Robo2* in the venous pole and later only with *Robo2* in the atria, no *Robo* receptor genes were detected in the ventricular myocardium of the heart (Fig. 2). Despite its favorite link with Robo receptors, Slit contains domains that suggest association with the extracellular-matrix receptors (Chedotal, 2007). Furthermore, recent study in *Drosophila* have proposed that Slit is localized on cardiac cells by association with Dystroglycan (Dg), a proteoglycan (Medioni et al., 2008), and possibly also with αPS3/βPS1 Integrin (MacMullin and Jacobs, 2006).

The absence of *Slit3* gene expression and protein in AVC myocardium suggested potential regulation by the T-box transcriptional repressors *Tbx2* and *Tbx3* that are restricted to nonchamber myocardium (Supp. Fig. S3B,C), where they repress the chamber transcriptional program (Habets et al., 2002; Christoffels et al., 2004b; Harrelson et al., 2004; Bakker et al., 2008; Mesbah et al., 2008). Therefore, we examined *Slit3* expression in mutant embryos deficient for *Tbx2* and *Tbx3*. In situ hybridization on stage-matched embryos revealed activation of *Slit3* in the AVC of E10.5 $Tbx2^{-/-}$ but not $Tbx3^{-/-}$ hearts (Supp. Fig. S4). This observation indicates that Tbx2 alone is sufficient to repress *Slit3* in the nonchamber myocardium of $Tbx3^{-/-}$ hearts, consistent with previous findings on other chamber-specific genes (Bakker et al., 2008; Mesbah et al., 2008). The T-box factor Tbx20 is essential for embryonic chamber formation through its negative regulation of *Tbx2* in the myocardium and endocardium (Cai et al., 2005; Singh et al., 2005; Stennard et al., 2005; Takeuchi et al., 2005). To test the hypothesis that ectopic Tbx2 expression may be able to repress *Slit3* in the forming heart, we analyzed *Slit3* expression in $Tbx20^{-/-}$ embryos. Mutant embryos showed severe cardiac abnormalities including rudimentary ventricular chambers that did not further differentiate (Stennard et al., 2005). We could not detect any *Slit3* expression in $Tbx20^{-/-}$ hearts at E9 (compare Fig. 5B,B′ with 5A,A′). Of interest, *Drosophila Slit* is also perturbed in the embryonic heart tube of *Tbx20*-ortho-log ($H15^{nmr}$) mutants (Qian et al., 2005), suggesting a high evolutionary conservation of this regulation pathway. We also examined *Slit3* expression in embryos misexpressing *Tbx2* throughout the embryonic heart under the control of the *XMLC2* promoter (*XMLC2-rtTA/tetO-Tbx2*; (Dupays et al., 2009). Consistent with our observation in $Tbx20^{-/-}$ embryos, *Slit3* expression was significantly reduced (Fig. 5C,C′). The residual weak expression of *Slit3* observed in these embryos may be explained by the mosaic expression of the transgene at this stage (Dupays et al., 2009). Moreover, we found three conserved T-box binding elements (TBEs; Kispert and Herrmann, 1993; Sinha et al., 2000) in the *Slit3* 5′ proximal promoters (Fig. 5D). The requirement of these TBEs for repression in the AVC and the complementary expression pattern between *Tbx2* (Supp. Fig. S3) and *Slit3* (Fig. 4B) prompted us to study the interaction of Tbx2 with the TBE motifs identified in the *Slit3* promoter using electrophoretic mobility shift assay (EMSA) experiments. Oligonucleotide probes corresponding to the three TBE motifs were used. Tbx2 bound to the wild-type TBE2

motif but not TBE1 and TBE3, because a shifted band was detected only in lanes 11 and 12 (Fig. 5E). However, when the EMSA was performed with a mutated TBE2 motif this binding was abolished (Fig. 5E). Together these results suggest that *Slit3* expression may be directly repressed by Tbx2 during AVC formation.

Conclusion

In this study, we have characterized Slit ligand and Robo receptor gene expression in the developing mouse heart. Our results suggest that Slit-Robo signaling, essential for morphogenesis of the *Drosophila* heart tube, may play roles in oriented cell growth during atrial and ventricular morphogenesis in vertebrates. Furthermore, we identify two upstream regulators of *Slit3* expression, the predominant Slit ligand expressed in the early mouse heart: analysis of *Slit3* expression in different mutant mouse embryos reveals that *Slit3* is restricted to the ventral wall of the linear heart tube by Nkx2-5 regulated mechanisms and excluded from AVC myocardium by the transcriptional repressor Tbx2.

EXPERIMENTAL PROCEDURES

Animals and Tissue Preparation

All experiments involving animals were performed in accordance with French guidelines on the care and use of laboratory animals. After death by CO_2 asphyxiation, embryo mice were removed from timed-pregnant CD1 or mutant mice. The day of vaginal plugging was defined as 0.5. Embryos were genotyped by polymerase chain reaction (PCR) using genomic DNA isolated from yolk sacs. The null alleles *Tbx2*^{tm1Pa}, *Tbx3*^{tm1Pa}, *Tbx20*^{lacZ}, and *Nkx2-5*^{gfp} (hereafter referred to as *Tbx2*$^{-}$, *Tbx3*$^{-}$, *Tbx20*$^{-}$, and *Nkx2-5*$^{-}$) were maintained on a mixed genetic background (Biben et al., 2000; Davenport et al., 2003; Harrelson et al., 2004; Stennard et al., 2005). Somites were counted for developmental staging and a sample of the yolk sac was taken for PCR genotyping using the following primers. *Tbx3*: the primers 5′-GGC CTC AAG TAG CTT GGA A-3′, 5′-AGG CCA ACA GAA GAG CAG A-3′, and 5′-CTA AGC CTG ATG GTG TGA G-3′ result in a 350 bp wild-type band and a 500 bp mutant band. *Tbx2*: the primers 5′-CCA GCC AGG GAA CAT AAT GAG G-3′, 5′-CTG TCC CCT GGC ATT TCT GG-3′, and 5′-CCT GCA GGA ATT CCT CGA CC-3′ result in a 180 bp wild-type band and a 88 bp mutant band. *Nkx2-5*: the primers 5′-GAA CCT GGA GCA GCA GCA GCG TAG C-3′ and 5′-CAG AAG GGA AGA GCT TGA GGT TCT C-3′ result in a 308 bp wild-type band and a 1,376 bp mutant band.

The tetO-Tbx2 and xMlc2-rtTA transgenes have been previously described (Dupays et al., 2009). Doxycycline was administered to pregnant females either by intraperitoneal injection (2 mg of Dox in 0.5 ml of 0.9% aqueous NaCl) at the indicated stage or by means of food (2 mg of Dox in 0.5 ml of 0.9% aqueous NaCl) from stages specified.

For early developmental stages whole embryos were fixed in 4% paraformaldehyde (PFA) in phosphate buffered saline (PBS) overnight at 4°C, dehydrated and kept in methanol. Hearts or trunks were dissected and fixed in 4% PFA in PBS overnight at 4°C, transferred to 15% sucrose in PBS, followed by 15% sucrose 7% gelatin, and frozen in liquid nitrogen before cryo-sectioning at 10 μm.

Whole-Mount In Situ Hybridization

Whole-mount in situ hybridization was carried out as published (Zaffran et al., 2004). Probes were labeled according to the manufacturer's instruction using the digoxigenin (DIG) -RNA labeling mix (Roche). The probes used for in situ hybridization were *mSlit2* and *mSlit3* (Yuan et al., 1999), rat *Slit1, Robo1, Robo2* (Kidd et al., 1998), *Rig1/Robo3*, and

mRobo4 3′-untranslated region (obtained by PCR). Hybridization signals were then detected by alkaline phosphatase (AP) -conjugated anti-DIG antibodies (1/2,000; Roche), which were followed by color development with NBT/BCIP (nitroblue tetrazolium/5-bromo-4-chloro-3-indolyl phosphate) substrate (Promega). After staining, the samples were washed in PBS and post-fixed. Embryos were imaged using a Zeiss Lumar stereomicroscope coupled to an Axiocam digital camera (AxioVision 4.4, Zeiss). The number of embryos examined was at least 3 for each stage.

Immunohistochemistry

For immunohistochemistry, sections were incubated as described previously (Zaffran et al., 2004). The Slit3 antibody, C-20, was a polyclonal antibody raised against a peptide mapping within an internal region of Slit3 of human origin from Santa Cruz, used at 1/50 dilution. The Robo1 and *Robo2* antibodies were polyclonal antibody raised against ectodomains of rat Robo1 (amino acids 1–892) and rat *Robo2* (amino acids 1–855) as described previously (Tamada et al., 2008). Secondary antibodies were donkey anti-goat or anti-rabbit, Alexa 488 used at 1/500 dilution (Molecular Probes). Sections were photographed using a Zeiss Axiovert 200M microscope with an Axiocam camera (AxioVision 4.4, Zeiss).

DNA-Binding Assay

For EMSA, the Tbx2 protein was produced with the TNT (T7) -coupled in vitro transcription/translation system (Promega). Production yields of Tbx2 protein was estimated by [^{35}S]methionine labeling. EMSAs were performed in a 20-µl volume on ice with 10^4 cpm (0.5 ng) of either probes. Probes used were double-stranded: TBE1 (5′-TTTTTGTGTGTGAAAGTGCA), TBE 1mut (5′-TTTTTGTcaaaGAAAGTGCA), TBE2 (5′-TAGTGATGGTGTCAATACCGG), TBE2mut (5′-TAGTGATGcaaaCAATACCGG), TBE3 (5′-TGCCTTAGCTGTGAACACTAAT) and TBE3mut (5′-TGCCTTAGCTcaatACACTAAT) from the *Slit3* promoter. Briefly, 3 or 9 µl of Tbx2 protein was gently added and incubated for 30 min with labeled probes and 0.1 mg of nonspecific competitor poly[(dC)] in a binding buffer 5× composition of 20% glycerol, 50 mM Tris-HCl pH7.5, 250 mM NaCl, 2.5 mM ethylenediaminetetraacetic acid, 2.5 mM dithiothreitol, and 0.25 mg BSA then loaded on a 4% polyacrylamide gel in 0.25× TBE buffer. The gel was dried and analyzed with a PhosphoImager.

Supplementary Material

Refer to Web version on PubMed Central for supplementary material.

Acknowledgments

We thank Dr. David Ornitz for his kind and generous gift of the *Slit2* and *Slit3* vectors, and Dr. Alain Chedotal for providing the *Slit1* and *Robo1, Robo2*, and *Robo3* vectors. We thank Dr. Fugio Murakami for generously providing Robo1 and *Robo2* antibodies. We are grateful to Dr. Samir Merabet for allowing Bruno Hudry to carry out part of this work. We thank Dr. Robert Kelly for discussion and comments on the manuscript. S.Z. was funded by grants from the “Agence Nationale pour la Recherche” and V.E.P. was funded by the NIH. K.M. was supported by the European Commission under the FP7 CardioGeNet project.

Grant sponsor: Agence Nationale pour la Recherche; Grant number: ANR-007-MRAR-003; Grant sponsor: NIH; Grant number: 5R37HD033082; Grant sponsor: The European Commission; Grant number: HEALTH-2007-B-223463.

REFERENCES

Bakker ML, Boukens BJ, Mommersteeg MT, Brons JF, Wakker V, Moorman AF, Christoffels VM. Transcription factor Tbx3 is required for the specification of the atrioventricular conduction system. Circ Res 2008;102:1340–1349. [PubMed: 18467625]

Biben C, Harvey RP. Homeodomain factor Nkx2-5 controls left/right asymmetric expression of bHLH gene eHand during murine heart development. Genes Dev 1997;11:1357–1369. [PubMed: 9192865]

Biben C, Weber R, Kesteven S, Stanley E, McDonald L, Elliott DA, Barnett L, Koentgen F, Robb L, Feneley M, Harvey RP. Cardiac septal and valvular dysmorphogenesis in mice heterozygous for mutations in the homeobox gene Nkx2-5. Circ Res 2000;87:888–895. [PubMed: 11073884]

Brose K, Bland KS, Wang KH, Arnott D, Henzel W, Goodman CS, Tessier-Lavigne M, Kidd T. Slit proteins bind Robo receptors and have an evolutionarily conserved role in repulsive axon guidance. Cell 1999;96:795–806. [PubMed: 10102268]

Buckingham M, Meilhac S, Zaffran S. Building the mammalian heart from two sources of myocardial cells. Nat Rev Genet 2005;6:826–835. [PubMed: 16304598]

Cai CL, Zhou W, Yang L, Bu L, Qyang Y, Zhang X, Li X, Rosenfeld MG, Chen J, Evans S. T-box genes coordinate regional rates of proliferation and regional specification during cardiogenesis. Development 2005;132:2475–2487. [PubMed: 15843407]

Calmont A, Ivins S, Van Bueren KL, Papangeli I, Kyriakopoulou V, Andrews WD, Martin JF, Moon AM, Illingworth EA, Basson MA, Scambler PJ. Tbx1 controls cardiac neural crest cell migration during arch artery development by regulating Gbx2 expression in the pharyngeal ectoderm. Development 2009;136:3173–3183. [PubMed: 19700621]

Camurri L, Mambetisaeva E, Sundaresan V. Rig-1 a new member of Robo family genes exhibits distinct pattern of expression during mouse development. Gene Expr Patterns 2004;4:99–103. [PubMed: 14678835]

Chedotal A. Slits and their receptors. Adv Exp Med Biol 2007;621:65–80. [PubMed: 18269211]

Christoffels VM, Habets PE, Franco D, Campione M, de Jong F, Lamers WH, Bao ZZ, Palmer S, Biben C, Harvey RP, Moorman AF. Chamber formation and morphogenesis in the developing mammalian heart. Dev Biol 2000;223:266–278. [PubMed: 10882515]

Christoffels VM, Burch JB, Moorman AF. Architectural plan for the heart: early patterning and delineation of the chambers and the nodes. Trends Cardiovasc Med 2004a;14:301–307. [PubMed: 15596106]

Christoffels VM, Hoogaars WM, Tessari A, Clout DE, Moorman AF, Campione M. T-box transcription factor Tbx2 represses differentiation and formation of the cardiac chambers. Dev Dyn 2004b;229:763–770. [PubMed: 15042700]

Davenport TG, Jerome-Majewska LA, Papaioannou VE. Mammary gland, limb and yolk sac defects in mice lacking Tbx3, the gene mutated in human ulnar mammary syndrome. Development 2003;130:2263–2273. [PubMed: 12668638]

de la Cruz, M.; Markwald, R., editors. Living morphogenesis of the heart. Boston: Birkhauser; 1999.

Dupays L, Kotecha S, Angst B, Mohun TJ. Tbx2 misexpression impairs deployment of second heart field derived progenitor cells to the arterial pole of the embryonic heart. Dev Biol 2009;333:121–131. [PubMed: 19563797]

Habets PE, Moorman AF, Clout DE, van Roon MA, Lingbeek M, van Lohuizen M, Campione M, Christoffels VM. Cooperative action of Tbx2 and Nkx2.5 1inhibits ANF expression in the atrioventricular canal: implications for cardiac chamber formation. Genes Dev 2002;16:1234–1246. [PubMed: 12023302]

Harrelson Z, Kelly RG, Goldin SN, Gibson-Brown JJ, Bollag RJ, Silver LM, Papaioannou VE. Tbx2 is essential for patterning the atrioventricular canal and for morphogenesis of the outflow tract during heart development. Development 2004;131:5041–5052. [PubMed: 15459098]

Harvey RP. Organogenesis: patterning the vertebrate heart. Nat Rev Genet 2002;3:544–556. [PubMed: 12094232]

Holmes G, Niswander L. Expression of slit-2 and slit-3 during chick development. Dev Dyn 2001;222:301–307. [PubMed: 11668607]

Holmes GP, Negus K, Burridge L, Raman S, Algar E, Yamada T, Little MH. Distinct but overlapping expression patterns of two vertebrate slit homologs implies functional roles in CNS development and organogenesis. Mech Dev 1998;79:57–72. [PubMed: 10349621]

Jia L, Cheng L, Raper J. Slit/Robo signaling is necessary to confine early neural crest cells to the ventral migratory pathway in the trunk. Dev Biol 2005;282:411–421. [PubMed: 15950606]

Kelly RG, Buckingham ME. The anterior heart-forming field: voyage to the arterial pole of the heart. Trends Genet 2002;18:210–216. [PubMed: 11932022]

Kidd T, Brose K, Mitchell KJ, Fetter RD, Tessier-Lavigne M, Goodman CS, Tear G. Roundabout controls axon crossing of the CNS midline and defines a novel subfamily of evolutionarily conserved guidance receptors. Cell 1998;92:205–215. [PubMed: 9458045]

Kidd T, Bland KS, Goodman CS. Slit is the midline repellent for the robo receptor in Drosophila. Cell 1999;96:785–794. [PubMed: 10102267]

Kirby, M., editor. Cardiac development. Oxford: Oxford University Press; 2007.

Kispert A, Herrmann BG. The Brachyury gene encodes a novel DNA binding protein. EMBO J 1993;12:3211–3220. [PubMed: 8344258]

Komuro I, Izumo S. Csx: a murine homeobox-containing gene specifically expressed in the developing heart. Proc Natl Acad Sci U S A 1993;90:8145–8149. [PubMed: 7690144]

Liu J, Zhang L, Wang D, Shen H, Jiang M, Mei P, Hayden PS, Sedor JR, Hu H. Congenital diaphragmatic hernia, kidney agenesis and cardiac defects associated with Slit3-deficiency in mice. Mech Dev 2003;120:1059–1070. [PubMed: 14550534]

Lyons I, Parsons LM, Hartley L, Li R, Andrews JE, Robb L, Harvey RP. Myogenic and morphogenetic defects in the heart tubes of murine embryos lacking the homeo box gene Nkx2-5. Genes Dev 1995;9:1654–1666. [PubMed: 7628699]

MacMullin A, Jacobs JR. Slit coordinates cardiac morphogenesis in Drosophila. Dev Biol 2006;293:154–164. [PubMed: 16516189]

Medioni C, Astier M, Zmojdzian M, Jagla K, Semeriva M. Genetic control of cell morphogenesis during Drosophila melanogaster cardiac tube formation. J Cell Biol 2008;182:249–261. [PubMed: 18663140]

Medioni C, Senatore S, Salmand PA, Lalevee N, Perrin L, Semeriva M. The fabulous destiny of the Drosophila heart. Curr Opin Genet Dev 2009;19:518–525. [PubMed: 19717296]

Meilhac SM, Esner M, Kerszberg M, Moss JE, Buckingham ME. Oriented clonal cell growth in the developing mouse myocardium underlies cardiac morphogenesis. J Cell Biol 2004;164:97–109. [PubMed: 14709543]

Mesbah K, Harrelson Z, Theveniau-Ruissy M, Papaioannou VE, Kelly RG. Tbx3 is required for outflow tract development. Circ Res 2008;103:743–750. [PubMed: 18723448]

Ong LL, Kim N, Mima T, Cohen-Gould L, Mikawa T. Trabecular myocytes of the embryonic heart require N-cadherin for migratory unit identity. Dev Biol 1998;193:1–9. [PubMed: 9466883]

Park KW, Morrison CM, Sorensen LK, Jones CA, Rao Y, Chien CB, Wu JY, Urness LD, Li DY. Robo4 is a vascular-specific receptor that inhibits endothelial migration. Dev Biol 2003;261:251–267. [PubMed: 12941633]

Qian L, Liu J, Bodmer R. Slit and Robo control cardiac cell polarity and morphogenesis. Curr Biol 2005;15:2271–2278. [PubMed: 16360689]

Santiago-Martinez E, Soplop NH, Patel R, Kramer SG. Repulsion by Slit and Roundabout prevents Shotgun/E-cadherin-mediated cell adhesion during Drosophila heart tube lumen formation. J Cell Biol 2008;182:241–248. [PubMed: 18663139]

Simpson JH, Kidd T, Bland KS, Goodman CS. Short-range and long-range guidance by slit and its Robo receptors. Robo and Robo2 play distinct roles in midline guidance. Neuron 2000;28:753–766. [PubMed: 11163264]

Singh MK, Christoffels VM, Dias JM, Trowe MO, Petry M, Schuster-Gossler K, Burger A, Ericson J, Kispert A. Tbx20 is essential for cardiac chamber differentiation and repression of Tbx2. Development 2005;132:2697–2707. [PubMed: 15901664]

Sinha S, Abraham S, Gronostajski RM, Campbell CE. Differential DNA binding and transcription modulation by three T-box proteins, T, TBX1 and TBX2. Gene 2000;258:15–29. [PubMed: 11111039]

Stennard FA, Costa MW, Lai D, Biben C, Furtado MB, Solloway MJ, McCulley DJ, Leimena C, Preis JI, Dunwoodie SL, Elliott DE, Prall OW, Black BL, Fatkin D, Harvey RP. Murine T-box transcription factor Tbx20 acts as a repressor during heart development, and is essential for adult heart integrity, function and adaptation. Development 2005;132:2451–2462. [PubMed: 15843414]

Strickland P, Shin GC, Plump A, Tessier-Lavigne M, Hinck L. Slit2 and netrin 1 act synergistically as adhesive cues to generate tubular bi-layers during ductal morphogenesis. Development 2006;133:823–832. [PubMed: 16439476]

Takeuchi JK, Mileikovskaia M, Koshiba-Takeuchi K, Heidt AB, Mori AD, Arruda EP, Gertsenstein M, Georges R, Davidson L, Mo R, Hui CC, Henkelman RM, Nemer M, Black BL, Nagy A, Bruneau BG. Tbx20 dose-dependently regulates transcription factor networks required for mouse heart and motoneuron development. Development 2005;132:2463–2474. [PubMed: 15843409]

Tamada A, Kumada T, Zhu Y, Matsumoto T, Hatanaka Y, Muguruma K, Chen Z, Tanabe Y, Torigoe M, Yamauchi K, Oyama H, Nishida K, Murakami F. Crucial roles of Robo proteins in midline crossing of cerebellofugal axons and lack of their up-regulation after midline crossing. Neural Dev 2008;3:29. [PubMed: 18986510]

Togi K, Kawamoto T, Yamauchi R, Yoshida Y, Kita T, Tanaka M. Role of Hand1/eHAND in the dorso-ventral patterning and interventricular septum formation in the embryonic heart. Mol Cell Biol 2004;24:4627–4635. [PubMed: 15143159]

Wu JY, Feng L, Park HT, Havlioglu N, Wen L, Tang H, Bacon KB, Jiang Z, Zhang X, Rao Y. The neuronal repellent Slit inhibits leukocyte chemotaxis induced by chemotactic factors. Nature 2001;410:948–952. [PubMed: 11309622]

Yuan W, Zhou L, Chen JH, Wu JY, Rao Y, Ornitz DM. The mouse SLIT family: secreted ligands for ROBO expressed in patterns that suggest a role in morphogenesis and axon guidance. Dev Biol 1999;212:290–306. [PubMed: 10433822]

Yuan W, Rao Y, Babiuk RP, Greer JJ, Wu JY, Ornitz DM. A genetic model for a central (septum transversum) congenital diaphragmatic hernia in mice lacking Slit3. Proc Natl Acad Sci U S A 2003;100:5217–5222. [PubMed: 12702769]

Zaffran S, Kelly RG, Meilhac SM, Buckingham ME, Brown NA. Right Ventricular Myocardium Derives From the Anterior Heart Field. Circ Res 2004;95:261–268. [PubMed: 15217909]

Zhang B, Dietrich UM, Geng JG, Bicknell R, Esko JD, Wang L. Repulsive axon guidance molecule Slit3 is a novel angiogenic factor. Blood 2009;114:4300–4309. [PubMed: 19741192]

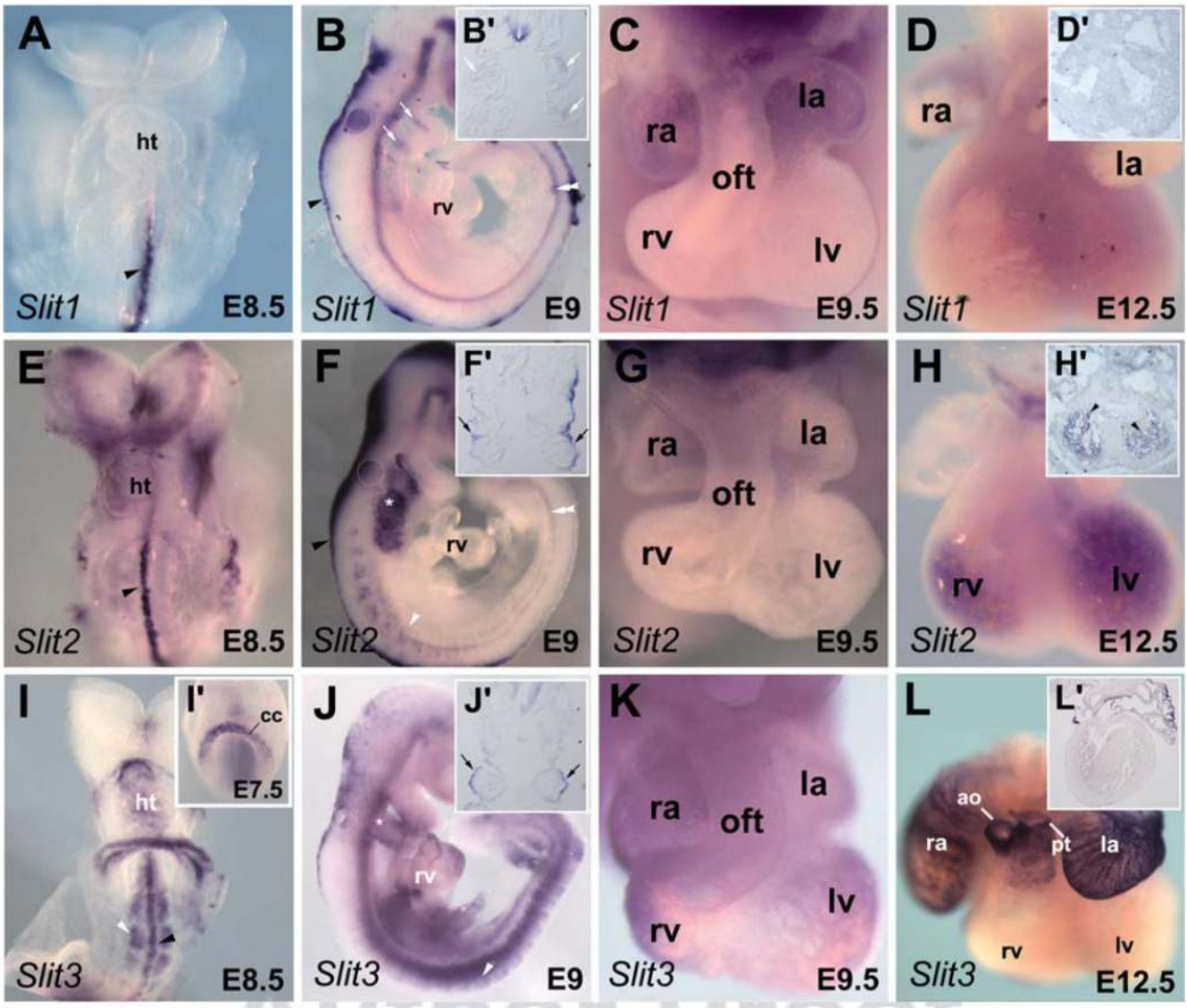

Fig. 1.

Expression pattern of *Slit* genes during embryonic heart development. Whole-mount in situ hybridization analysis of embryos with *Slit1* (A–D), *Slit2* (E–H), and *Slit3* (I–L) probes. **A:** Ventral view of embryonic day (E) 8.5 embryo showing *Slit1* expression in the ventral midline (arrowhead). *Slit1* is not detected in the forming heart tube. **B:** Lateral view of E9 embryo showing *Slit1* expression in the roof plate (arrowhead), in the floor plate (double arrowhead), and the pharyngeal region (white arrows). **B′:** Frontal section (same embryo depicted in B) showing *Slit1* expression in the mesodermal core of the pharyngeal arch (white arrows) and in the floor plate of the spinal cord. **C:** High magnification picture of heart at late E9.5 showing *Slit1* in atrial wall. **D:** Dissected E12.5 heart showing no expression of *Slit1*. **D′:** In situ hybridization with *Slit1* on section of E12.5 heart. **E:** *Slit2* was not detected in the heart of embryo at E8.5 stage. Note its expression at the ventral midline (arrowhead). **F:** Lateral view of early E9.5 embryo showing *Slit2* expression in the pharyngeal region (asterisk). *Slit2* is also detected in the roof plate (arrowhead), the notochord (double arrowheads) and the somites (white arrowhead). **F′:** Frontal section (same embryo depicted in F) showing *Slit2* expression in the pharyngeal ectoderm surface

(arrows). **G:** Dissected E9.5 heart showing no expression of *Slit2*. **H:** A robust expression of *Slit2* is detected in trabeculae of both ventricles at E12.5. **H′:** In situ hybridization on section of E12.5 heart shows expression in the trabeculae (arrowhead). **I,I′:** Ventral views of E7.5 and E8.5 embryos showing *Slit3* expression in the cardiac crescent and the forming heart tube. Expression of *Slit3* is also detected in the ventral midline (black arrowhead) and the somites (white arrowhead) of E8.5 embryo. **J:** Lateral view of early E9.5 embryo showing *Slit3* expression in the heart and the pharyngeal ectoderm surface (asterisk) and in the somites (white arrowhead). **J′:** Frontal section (same embryo depicted in J) showing expression of *Slit3* the pharyngeal ectoderm surface (arrows). **K:** High magnification picture of the heart at late E9.5. Expression of *Slit3* is seen in the outflow tract, the atria and ventricles of the embryonic heart. **L:** At E12.5, expression of *Slit3* is maintained in the right and left atria and in great arteries, the aorta and pulmonary trunk. **L′:** Section of the heart shown in L. ao, aorta; cc, cardiac crescent; ht, heart tube; la, left atrium; lv, left ventricle; oft, outflow tract; pt, pulmonary trunk; ra; right atrium; rv, right ventricle.

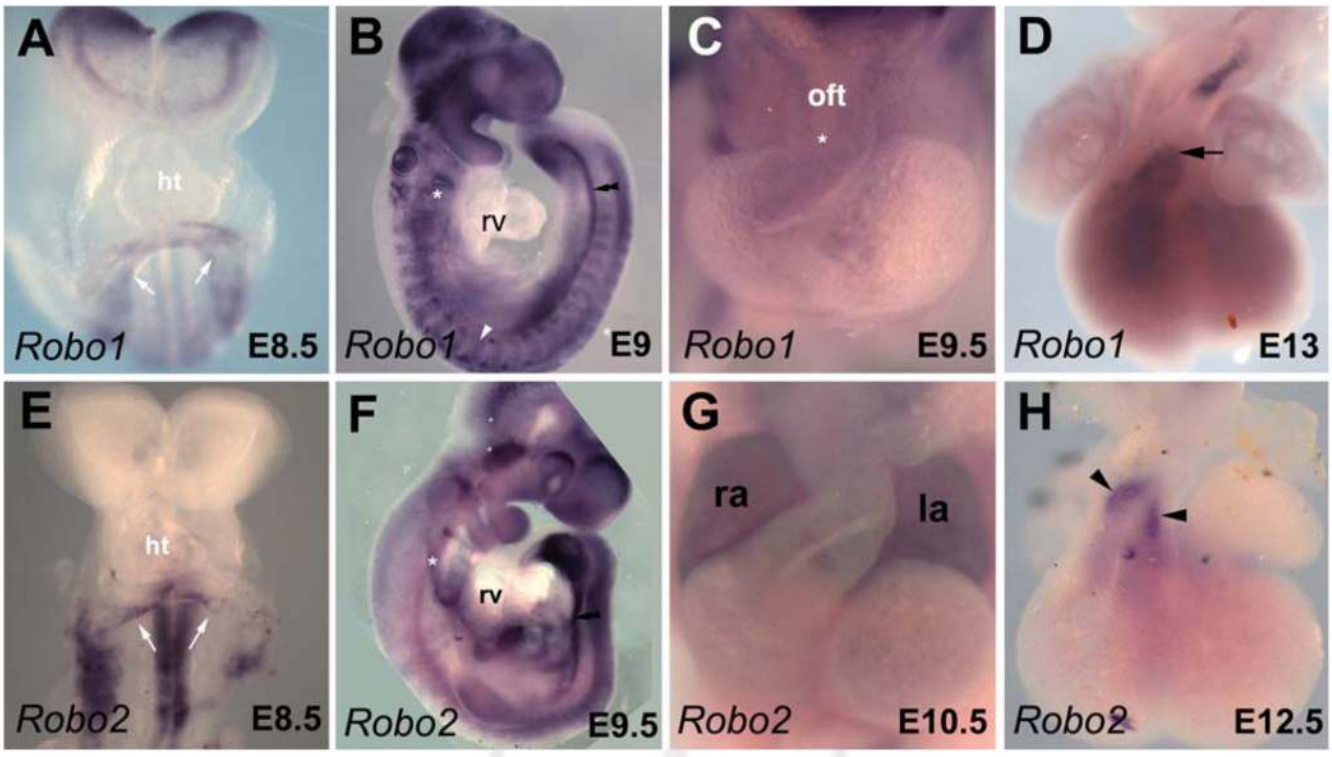

Fig. 2.

Expression pattern of *Robo* genes during embryonic heart development. Whole-mount in situ hybridization analysis of embryos with *Robo1* (A–D) and *Robo2* (E–H) probes. **A:** Ventral view of early embryonic day (E) 8.5 embryo showing *Robo1* expression in the venous pole (white arrows) of the forming heart tube. **B:** Lateral view of early E9 embryo. *Robo1* expression is detected in the notochord (double arrowhead), the somites (white arrowhead), and the ectodermal pouches of the pharyngeal arches (asterisk) but not in the heart. **C:** High magnification picture of the heart at late E9.5 showing *Robo1* in the cushions (asterisk) of the outflow tract. **D:** Dissected E12.5 heart showing expression of *Robo1* at the base of the great arteries (arrow). **E:** Ventral view of early E8.5 embryo. High Robo2 expression levels are visible in the neural tube and the venous pole (white arrows) of the forming heart tube. **F:** Lateral view of E9.5 embryo. Weak expression of *Robo2* is detected in the looped heart, the ectoderm of the pharyngeal arches (asterisk) and the notochord (double arrowheads). **G:** High magnification of the heart at E10.5 showing *Robo2* in both atria. **H:** Dissected E12.5 heart showing expression of *Robo2* in the great arteries (arrowheads). ht, heart tube; la, left atrium; lv, left ventricle; oft, outflow tract; ra; right atrium; rv, right ventricle.

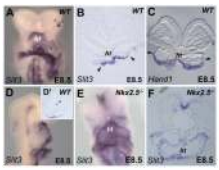

Fig. 3.

Dorsoventral patterning of *Slit3* expression in the linear heart tube requires Nkx2-5. **A:** Ventral view of embryo at early embryonic day (E) 8.5. *Slit3* is highly expressed in the ventral side of the forming heart tube. **B:** Section (same embryo as depicted in A) showing that *Slit3* expression in the heart tube is strictly ventral as delimited by the arrowheads. **C:** Expression of *Hand1* is shown as a reference to indicate the ventral side (arrowheads) of the heart tube at E8.5. D,E: Comparison of *Slit3* expression in wild-type (WT) and *Nkx2-5*$^{-/-}$ embryos at E8.5. **D:** Lateral view of WT embryo showing high expression of *Slit3* in the ventral side of the forming heart tube. **D′:** Section of the embryo shown in D. Note the expression of *Slit3* in the floor plate (arrow). **E:** Slit3 expression is maintained in *Nkx2-5*$^{-/-}$ embryo. **F:** Section (same embryo as shown in E) reveals that *Slit3* is uniformly expressed in heart of *Nkx2-5*$^{-/-}$ embryo. ht, heart tube; nt, neural tube.

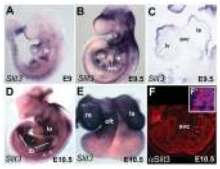

Fig. 4.

Dynamic expression pattern of *Slit3* during heart development. In situ hybridization (A–E) and immunofluorescence (F) were used to detect spatial expression of Slit3 in hearts from embryonic day (E) 9 to E10.5. **A,B:** Expression of *Slit3* is detected in the whole heart of E9 embryo, whereas it is down-regulated in the AVC of late E9.5 embryo. **C:** Section (same embryo as depicted in B) showing expression of *Slit3* in the chambers but not in the AVC. Note weak expression of *Slit3* in the trabeculae of the left ventricle. **D:** Lateral view of E10.5 embryo. High expression of *Slit3* is detected in the left atrium. Note *Slit3* expression in the limb buds and the dermomyotome (white arrowheads). **E:** Dissected heart from the embryo shown in D. High expression is observed in the right and left atria and the outflow tract. **F:** Expression of Slit3 protein (red) is detected in the ventricular myocardium and trabeculae but not in the AVC of heart at E10.5. Higher magnification of the trabeculae region delimited by the dotted line is shown in the inset. **F′:** Immunodetection of Slit3 (red) and DAPI (blue) staining. Note Slit3 expression in the cytoplasm. ao, aorta; avc, atrioventricular canal; la, left atrium; lb, limb bud; lv, left ventricle; oft, outflow tract; pt, pulmonary trunk; ra, right atrium; rv, right ventricle.

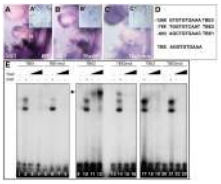

Fig. 5.

Disrupted cardiac expression of *Slit3* in *Tbx20* mutant and in *Tbx2*-misexpression embryos. **A–C:** Lateral views of wild-type (WT), *Tbx20*$^{-/-}$ mutant and *Tbx2*-misexpressing embryos. **A′–C′:** Sections of embryos shown in A–C. While *Slit3* is present in the forming heart of WT embryo (A,A′), its expression is not detected in the heart of E9 *Tbx20*$^{-/-}$ embryo (B,B′). C,C′: *Slit3* expression is highly reduced in heart misexpressing *Tbx2*. **D:** Sequence of three-conserved T-box binding elements (TBE) found in a *Slit3* 5′ proximal promoter. Numbers indicate position of the sequences from the ATG. TBE sequence shows the T-box binding site as determined previously (Kispert and Herrmann, 1993). **E:** Electrophoretic mobility shift assay shows that Tbx2 binds to the wild-type TBE2 motif (lanes 9–12) but not to the TBE1 (lanes 1–8) and TBE3 (lanes 17–23) motifs. Mutation of the TBE2 motif impairs Tbx2 binding (lanes 13–16). la, left atria; lv, left ventricle.